Novel real-time alignment and calibration of LHCb detector for Run II and tracking for the upgrade.

Renato Quagliani[1,2] **on behalf of the LHCb collaboration**
[1]Laboratoire de l'Accelerateur Lineare, Orsay, France
[2]Bristol University, Bristol, United Kingdom

E-mail: `rquaglia@cern.ch`

Abstract. LHCb has introduced a novel real-time detector alignment and calibration strategy for LHC Run II. Data collected at the start of the fill is processed in a few minutes and used to update the alignment, while the calibration constants are evaluated for each run. The procedure aims to improve the quality of the online selection and performance stability. The required computing time constraints are met thanks to a new dedicated framework using the multi-core farm infrastructure for the trigger. A similar scheme is planned to be used for Run III foreseen to start in 2020. At that time LHCb will run at an instantaneous luminosity of 2×10^{33} cm^{-2} s^{-1} and a fully software based trigger strategy will be used. The new running conditions and the tighter timing constraints in the software trigger (only 13 ms per event are available) represent a big challenge for track reconstruction. The new software based trigger strategy implies a full detector read-out at the collision rate of 40 MHz. High performance and timing constraints are ensured by a new tracking system and a fast and efficient track reconstruction strategy.

1. Introduction

The LHCb detector [1] is a single-arm forward spectrometer covering a pseudorapidity range $1.9 < \eta < 4.9$ designed to study CP-violating processes and decay modes of hadrons containing b and c quarks which are highly suppressed in the Standard Model. The physics goals of LHCb are achieved thanks to an excellent tracking and particle identification (PID) system [2].

The LHCb tracking system is composed by three main detectors: a silicon-strip vertex detector (VELO) surrounding the pp interaction aiming to identify primary (PV) and secondary (SV) vertices, a large-area silicon strip detector (TT) consisting of four layers placed upstream the dipole magnet (4 Tm bending power) and three stations (four layers per station) of silicon-strip detectors (IT, in the inner region[1]) and straw drift tubes (OT, in the outer region) [4] downstream the dipole magnet.

Particle identification is achieved thanks to two ring-imaging Cherenkov (RICH1 and RICH2) detectors [5] placed upstream and downstream the magnet. Electrons, photons and hadrons are identified by the electromagnetic (ECAL) and hadronic (HCAL) calorimeter system [6]. Muons are identified by five muon tracking stations made of multi-wire proportional chambers alternated with layers of iron [7].

A sketch of the LHCb trigger strategy for Run I, Run II and the one foreseen for the upgrade phase in 2020 are summarized in Fig 1. Events are selected by a trigger consisting of a hardware

[1] Closer to the beam pipe

Table 1: Run I and Run II timing budget comparison in the HLT.

Trigger step	Output rate (Run I $\rightarrow$ Run II)	Time budget (Run I $\rightarrow$ Run II)
HLT1	(80 $\rightarrow$ 150) kHz	(20 $\rightarrow$ 35) ms/event
HLT2	(5 $\rightarrow$ 12.5) kHz	(150 $\rightarrow$ 650) ms/event

stage (L0) aiming to reduce the event rate to the maximal read-out rate of tracking sub-detectors of 1 MHz using solely information from muon stations and calorimeters, followed by a software stage (HLT)[2]. HLT is divided in two steps, HLT1 and HLT2 performing a partial and a full event reconstruction, respectively.

The larger timing budget for both the HLT stages (see Table 1) available in Run II allows the introduction of the real-time detector alignment and calibration procedure taking advantage of the multi-core infrastructure of the Event Filter Farm (EFF). Furthermore, the full offline event reconstruction (used in Run I) becomes available in the HLT2 without any performance losses. Those factors combined together boost the physics performance of the apparatus, minimizing the online and offline selection performance. It also allows to apply exclusive selections at trigger level (mainly taking advantage of the full calibration of the PID system) reducing the output rate. Furthermore, by using directly the trigger output to perform physics analysis, large amount of disk space ($\sim$ 90%) is saved. LHC Run III will be characterized by a centre-of-mass energy of colliding protons equal of 14 TeV (7 and 8 in Run I, 13 in Run II), with a bunch spacing of 25 ns (was 50 ns for Run I) and the LHCb instantaneous luminosity will be $2 \times 10^{33}\,\mathrm{cm}^{-2}\ \mathrm{s}^{-1}$, almost a factor 5 higher with respect to Run I and Run II. This will improve the current sensitivity of the key measurements, e.g. $2\beta_s$,γ, $\mathcal{B}(B_s \rightarrow \mu^+\mu^-)$, charm CPV search and photon polarisation in exclusive $b \rightarrow s\gamma^{(*)}$, by almost a factor 10 [8].

In Run III, a higher detector occupancy, track multiplicity and pile-up[3] is expected together with a more complex event topology which requires an efficient and more sophisticated trigger selection, especially for hadronic decay modes. If the current (Run I and Run II) read-out limit of the tracking system of 1 MHz would be kept, it would imply tighter cuts in the L0 trigger, reducing the yield for hadronic modes. For such reasons, the LHCb detector will be upgraded: the entire detector will be read-out at 40 MHz and a fully software-based trigger [9] performing tracking at the collision rate will be used. The tracking strategy for the upgrade will benefit from the upgraded tracking system described in Sec. 3. Critically, the full software-based trigger implies tighter timing constraints (estimated to be $\sim$ 13 ms per event) which are met by the upgrade tracking strategy described in Sec. 3.1.

2. Real-time alignment and calibration at LHCb

Sub-detector alignment and calibration constants are evaluated at regular intervals, *i.e.*, per fill, per run or even less frequently. A dedicated data sample for each sub-detector calibration and alignment task is collected with specific trigger selections from the HLT1 and the updated alignment and calibration constants become available in a few minutes.

If the automatic procedure finds a significant variation of the constants with respect to the ones used previously (each run has a baseline set of constants), a new run is triggered and the updated constants are used in the trigger (HLT1 and HLT2) and for the further offline processing. Otherwise, the events are processed with the baseline ones.

[2] The hardware stage will be removed for the upgrade.

[3] The expected pile-up in Run III is 7.6, three times larger than Run I and Run II.

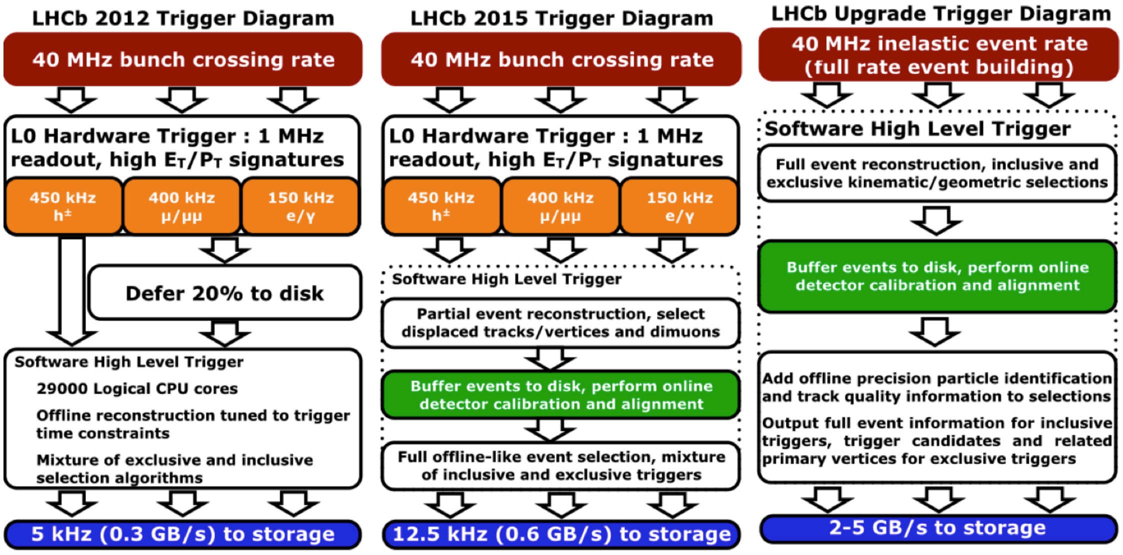

Figure 1: Diagrams of the LHCb trigger data-flow in Run I (left), Run II (center) and the one foreseen for Run III (right).

2.1. Framework

Two main activities are defined: alignment and calibration. The former benefits from the multi-core infrastructure of the EFF while the latter are mainly executed on a single node of the EFF (exception is done for the π^0 calorimeter calibration). The coordination of the different activities is guaranteed by a dedicated framework which exploits the multi-core infrastructure computing power. The framework is composed by the analyser, performing a massive parallelized (on ~ 1700 nodes) track reconstruction based on the alignment constants provided by the iterator. The iterator, running on a single node collects the analyser output and evaluate the constants for the next iteration. Depending on the task, the constants are evaluated in different ways: minimizing a Kalman filter fit χ^2 calculated from the residuals of reconstructed tracks for the tracking system alignment, and/or fitting monitoring histograms as it will be discussed later. The iterative procedure is interrupted when the variation of the χ^2 and/or the fit quality of the monitoring histograms are below a given threshold.

2.2. VELO, trackers and muon system alignment

The tracking system alignment is evaluated every fill. It is based on the minimization of a Kalman filter fit χ^2 calculated from the residual of already reconstructed tracks [10] [11]. The Kalman filter fit allows to include multiple scattering, energy loss and magnetic field effects and to provide multiple sub-detectors alignment at once. Moreover, mass and vertex constraints can be used to avoid global distorsion of the resulting alignment constants. Each sub-detector element constant is constrained to the nominal, surveyed or previously aligned position and the iterative alignment procedure to compute the updated alignment constants are stopped when the χ^2 variation is below threshold.

The VELO consists of two movable detector halves and it is the sub-detector closest to the interaction point (7.0 mm from beam pipe). During the LHC beam injection it is placed at a safe distance from the beam moving the two halves. Therefore, VELO alignment constants (3 translation and 3 rotation constants for each of the 86 detector elements) can change every fill.

The precision of the track based alignment procedure is $\mathcal{O}(2\mu\text{m})$ and the average observed misalignment of the VELO during Run I was 4μm with a maximum variation of $\mathcal{O}(10\mu\text{m})$. In

Fig. 2 one can see the stability of the VELO alignment during the data taking period in 2015 for the x and y translation constants (no relevant z translation is expected during data-taking).

The alignment constants are updated and a new Run is triggered only when the variation between the initial alignment constants and the ones evaluated by the automatic procedure is above threshold (black dashed line in Fig. 2). The full (empty) markers in Fig. 2 correspond to fills where a new run is (not) triggered.

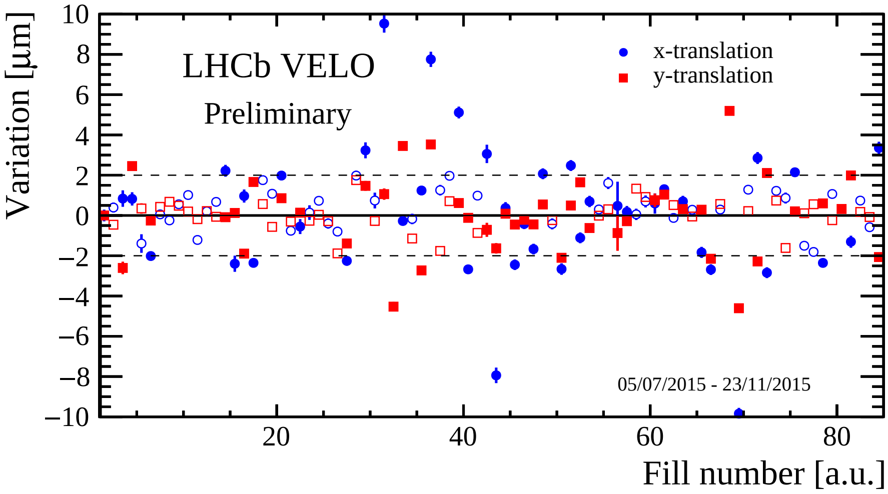

Figure 2: Stability of the alignment for translations in x and y direction of the VELO halves during Run II fills. On the y axis the difference between the initial alignment constant and the one computed by the automatic procedure.

Alignment of the trackers (upstream and downstream ones) is executed every fill after the VELO alignment. The constants might change during data taking due to magnet polarity switches, thus updates of the constants are expected every few weeks. Alignment constants for the muon stations are not expected to vary in time and the alignment procedure output is used as monitoring.

2.3. RICH mirror alignment

The RICH mirror alignment is executed every one or two fills and it is used as monitoring. It relies on the parallelized track reconstruction and the Cherenkov rings reconstruction on the Hybrid Photon Detector (HPD) plane. Both the tasks are performed by the analyser while the fit to the analyser output histograms to evaluate the alignment constants is performed by the iterator.

The Cherenkov light produced by particles entering the RICH radiators is reflected by a spherical and a flat mirror to the HPD plane. Therefore, the Cherenkov light cone produced is detected as a ring (with radius equal to the Cherenkov opening angle θ_{Ch}) centered at the intersection point of the incoming track with radiator material. Misalignment of the mirrors implies the observed Cherenkov ring center to be shifted by a quantity $\Delta\theta_{Ch}$ with respect to the expected position from tracking. The projected reconstructed track coordinate will then not correspond to the observed Cherenkov ring center. Therefore, the Cherenkov opening angle varies as a function of the azimuthal angle (ϕ) in the HPD plane. Misalignment of mirrors are encoded in the values of θ_x and θ_y which can be fitted for using $\Delta\theta_{Ch} = \theta_{Ch} - \theta_0 = \theta_x \cdot \cos\phi + \theta_y \cdot \sin\phi$, where θ_0 is the Cherenkov angle calculated from the momentum of the selected tracks of a given unambiguous PID assignment from other sub-detectors and from the refractive index of the radiator.

Fig. 3 shows $\Delta\theta_{Ch}(\phi)$ before and after the alignment procedure together with the stability of the Cherenkov angle resolution for RICH during 2015 data taking period.

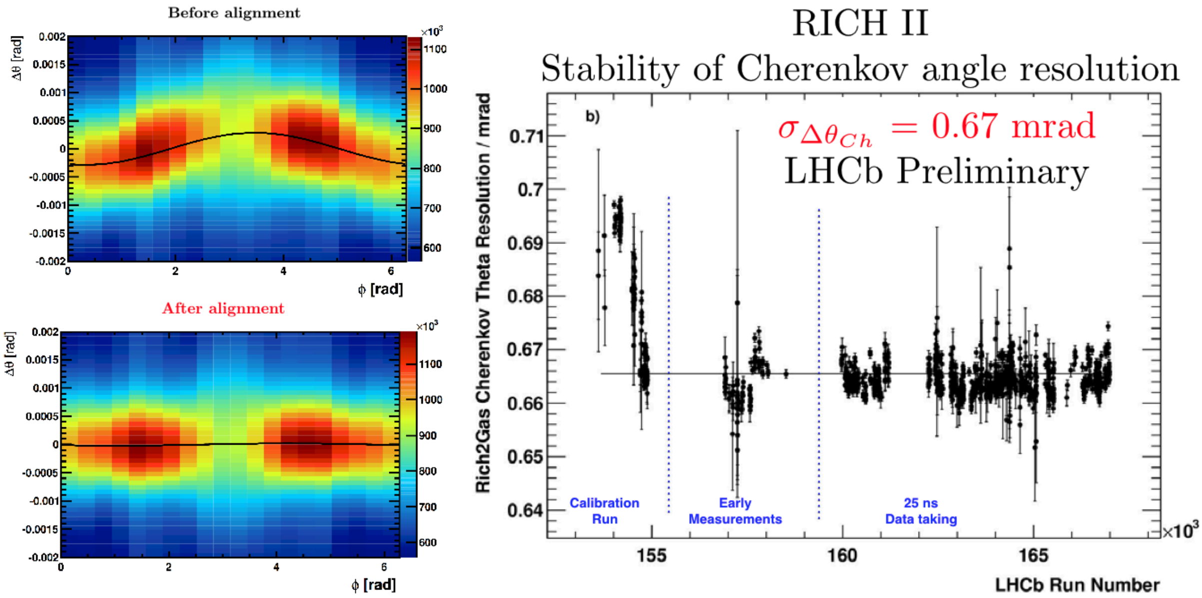

Figure 3: On the left the distribution of $\Delta\theta_{Ch}(\phi)$ used for the RICH mirrors alignment. On the right the stability of the Cherenkov angle resolution for RICH2 during 2015 data taking period.

2.4. Online calibration for RICH, OT and calorimeters

The HLT1 output of the online reconstruction and monitoring histograms is used to calibrate the RICH, OT timing offset t_0 and the calorimeter systems.

PID performance depends on the variation of the gas admixture, temperature and pressure of RICH radiators since they imply a variation of the refractive index of the radiators. At each run a fit for the difference between the reconstructed and the expected Cherenkov angle is performed and scale factors for the refractive index corrections are extracted.

The distance between the reconstructed track position and the wire position in the OT is proportional to the known drift time. Therefore a global offset of the drift time residual distribution for OT hits is used to correct the time-offset t_0 of read-out electronics with respect to the LHCb clock (relative to the time of collision). The calibration is performed every run and the t_0 offset constant is updated if the observed shift is above a given threshold.

Calorimeter calibration is achieved through relative and absolute methods consisting of adjustments of the photomultipliers (PMTs) HV settings. The relative method consists of a per-fill LED monitoring system aiming to detect aging of PMTs and it is performed for both ECAL and HCAL. The absolute method uses a reconstructed di-photons invariant mass spectrum peaking around the π^0 nominal value. Per-cell calibration coefficients are computed in order to shift as close as possible the π^0 reconstructed invariant mass to its nominal value.

Every technical stop a ^{137}Cs source scan is also performed to provide an absolute calibration of the HV settings for the PMTs.

3. LHCb upgrade

The whole tracking system will be upgraded for Run III. The current VELO will be substituted by a new design, consisting of hybrid pixel sensors placed at 5.1 mm from the beam-pipe [12].

From tracking point of view, the single hybrid pixel sensor has the benefit to provide directly an (x, y, z) measurement, leading to a more efficient, faster and simpler track reconstruction in the VELO. In fact, the magnetic field is negligible in the VELO region, thus VELO tracks are straight lines which are used as input for other pattern recognition algorithm. The trackers upstream and downstream the magnet will be substituted [13]. The upstream one will consists of four layers of large area silicon detector with a higher granularity and covering a larger acceptance in the central region. The downstream tracker, currently made of 3 stations (4 layers each for a total of 12 layers) of composite technologies will be fully replaced by a homogeneous scintillating fiber detector (SciFi) made of 2.5 m long vertically oriented fibers read-out by silicon photomultipliers.[4]. This technology solution guarantees a fast read-out of the detector at 40 MHz, a single hit position resolution in all the SciFi acceptance of σ_{x-z} ~100μm and a simpler and faster detector treatment from a tracking point of view.

3.1. Fast track reconstruction strategy in LHCb 2020 HLT

The online tracking in the first step of the HLT needs to match the timing requirements and efficiently select interesting events. The main steps for the online tracking sequence in LHCb 2020 HLT trigger [9] are summarized in Fig. 4.

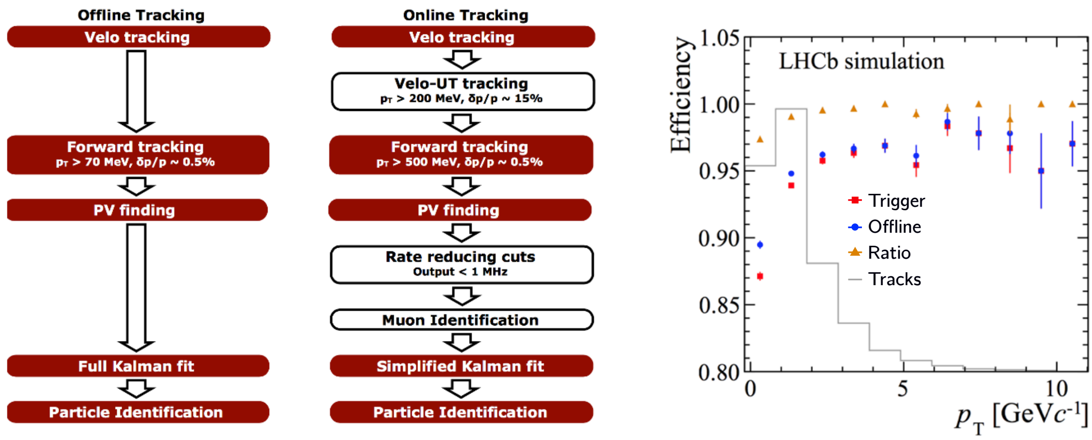

Figure 4: Online and offline tracking sequence comparison for the LHCb upgrade trigger (left). Online and offline tracking performance comparison as a function of the transverse momentum p_T of tracks (right). On the right also the transverse momentum distribution of tracks (in arbitrary scale) in a typical LHCb event is shown (gray line).

The main track reconstruction steps are:

(i) Velo tracking : segments in the VELO are looked for.

(ii) Velo-UT tracking : each segment is matched with a list of hits in the upstream tracker.

(iii) Forward tracking : VELO segments combined with the hits in the upstream tracker are used to look for matching segments in the SciFi.

(iv) PV finding: using the reconstructed tracks, PVs are searched for.

Velo-UT tracking allows to perform a momentum estimation (with $\frac{\delta p}{p} \sim 15\%$) and charge assignment which can be used to extrapolate the track in the downstream tracker and reduce the search windows, and thus the timing. The Forward tracking uses the momentum estimation and the charge information from VELO-UT tracking output to find matching segments in the

[4] Fibers are mirrored at $y = 0$, where y is the direction of the $\overrightarrow{B}$ field lines and z is the beam pipe direction.

SciFi. Each VELO segment is extrapolated to the SciFi stations and in each one of the 12 layers a search window is defined in order to collect the compatible hits, achieved thanks to a fast Hough transformation procedure [14]. The fast track reconstruction sequence combined with the upgraded tracking system is expected to find 98.7 % of the tracks which would be found by the slower offline sequence where no momentum requirements are added to the pattern recognition algorithms. The timing budget of 13 ms per event per single CPU is also satisfied, since the tracking sequence (VELO, VELO-UT, forward tracking and PV finding) takes 5.4 ms per event leaving the remaining timing budget for the leftover tasks. Events selected in this first fast partial event reconstruction will be used to feed the online alignment and calibration and the full event reconstruction at the reduced rate will be performed in a similar way as for Run II.

4. Summary

For Run II LHCb has implemented a fully automatic tracking system alignment and PID system alignment and calibration. Moreover, track and event reconstruction is fully performed in the online system relying on a fully calibrated and aligned system. This is possible thanks to the described dedicated framework developed for real-time alignment and calibration and the tracking timing improvements which allow to move the offline track reconstruction into the online system. In few minutes LHCb evaluates the updated calibration and alignment constants and the trigger output can be directly used to perform physics analysis.

For Run III data-taking, LHCb will upgrade the entire tracking system. The whole apparatus will be read-out at the collision rate and track reconstruction will be performed in real-time. The new tracking system and the fast tracking strategy described is expected to fit in the timing budget and guarantee high performance for the upgrade phase. Work is ongoing to improve the timing by exploiting possible new hardware architectures and to further improve the performances of tracking algorithms.

References

[1] Alves Jr A A *et al.* (LHCb) 2008 *JINST* **3** S08005

[2] Aaij R *et al.* (LHCb) 2015 *Int. J. Mod. Phys.* **A30** 1530022 (*Preprint* `1412.6352`)

[3] Aaij R *et al.* (LHCb) 2014 *JINST* **9** 09007 (*Preprint* `1405.7808`)

[4] Arink R *et al.* (LHCb Outer Tracker Group) 2014 *JINST* **9** P01002 (*Preprint* `1311.3893`)

[5] Adinolfi, M and others (LHCb RICH Group) 2013 *Eur. Phys. J.* **C73** 2431 (*Preprint* `1211.6759`)

[6] LHCb Collaboration 2000 LHCb calorimeters: Technical design report, *CERN-LHCC-2000-036*

[7] Alves, Jr, A A and others 2013 *JINST* **8** P02022 (*Preprint* `1211.1346`)

[8] LHCb Collaboration 2011 Letter of Intent for the LHCb Upgrade, *CERN-LHCC-2011-001*

[9] LHCb Collaboration 2014 LHCb Trigger and Online Upgrade Technical Design Report, *CERN-LHCC-2014-016*

[10] Hulsbergen, Wouter 2009 *Nucl. Instrum. Meth.* **A600** 471–477 (*Preprint* `0810.2241`)

[11] Amoraal J *et al.* 2013 *Nucl. Instrum. Meth.* **A712** 48–55 (*Preprint* `1207.4756`)

[12] LHCb Collaboration (LHCb) 2013 LHCb VELO Upgrade Technical Design Report, *CERN-LHCC-2013-021*

[13] LHCb Collaboration 2014 LHCb Tracker Upgrade Technical Design Report, *CERN-LHCC-2014-001*

[14] Amhis, Y and Callot, O and De Cian, M and Nikodem, T 2014 Description and performance studies of the Forward Tracking for a scintilating fibre detector at LHCb, *LHCb-PUB-2014-001*